

Axial behavior of steel-jacketed concrete columns

J. Rupp, H. Sezen^{*} and S. Chaturvedi

*The Ohio State University, Department of Civil, Environmental and Geodetic Engineering,
470 Hitchcock Hall, 2070 Neil Avenue, Columbus, Ohio, USA*

(Received November 25, 2012, Revised September 05, 2013, Accepted September 18, 2013)

Abstract. A new concrete confinement model is developed to predict the axial load versus displacement behavior of circular columns under concentric axial load. The new confinement model is proposed for concrete filled steel tube columns as well as circular reinforced concrete columns with steel tube jacketing. Existing confinement models were evaluated and improved using available experimental data from different sets of columns tested under similar loading conditions. The proposed model is based on commonly used confinement models with an emphasis on modifying the effective confining pressure coefficient utilizing the strength of the unconfined concrete and the steel tube, the length of the column, and the thickness of the steel tube. The proposed model predicts the ultimate axial strength and the corresponding strain with an acceptable degree of accuracy while also highlighting the importance of the manner in which the steel tube is used.

Keywords: confinement; concrete filled steel tube; axial strain; circular column; axial strength

1. Introduction

Concrete filled steel tubes have been popular in construction of various structures including bridges. Research by Knowles and Park (1969), Zhong and Miao (1987), Giakoumelis and Lam (2004), Gupta *et al.* (2007), Sakino *et al.* (2004), Sezen and Shamsai (2008), and Hatzigeorgiou (2008) examined the behavior of concrete filled tubes under concentric axial loading over the entire cross section while this research focuses on axial behavior of steel tubes filled with unreinforced and reinforced concrete, and existing concrete columns jacketed with steel tube. The process of strengthening structural members as a result of change of use or due to damage is common in structural engineering. In addition, existing structural members go through deterioration over the lifespan of a concrete structure caused by human activity or by environmental effects resulting in corrosion of steel bars or cracking and spalling of concrete. Rather than replacing these existing structural members, it can be more efficient to repair and strengthen them with a new confining material, such as steel, to provide an additional confinement mechanism.

Influenced by the experimental research of Sezen and Miller (2011), the purpose of this research is to use the principles of mechanics for confinement to propose stress-strain confinement

^{*}Corresponding author, Associate Professor, E-mail: sezen.1@osu.edu

^a M.S., E-mail: rupp.john@gmail.com

^b Associate Professor, E-mail: chaturvedi.1@osu.edu

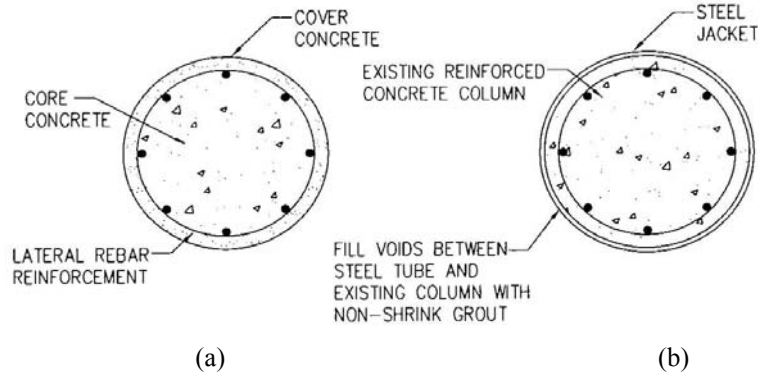


Fig. 1 (a) Cross section of a typical concrete column; and (b) with a steel tube jacket

models to account for the simultaneous presence of steel rebar in a concrete-filled steel tube column or a concrete column wrapped with a steel tube jacket. When the concrete is confined by lateral steel rebar, the strength of the confined concrete increases due to the lateral rebar resisting lateral expansion. In this research, concrete-filled steel tubes and steel jacketed columns are analyzed with steel thicknesses ranging from 1 mm to 6 mm and with yield strengths from 185 MPa to 360 MPa.

One of the main functions of the lateral reinforcement in the column in Fig. 1(a) is to confine the core concrete under concentric axial loading. The steel tube in Fig. 1(b) surrounding the column acts as additional lateral reinforcement and confines both the core and cover concrete. The compressive forces on the column will create lateral expansion of concrete that is fully confined by the steel tube allowing for larger axial load capacity. In addition, the steel tube can act as extra longitudinal reinforcement if any axial stress is transferred to the steel tube. There are several well established models to model concrete confined by transverse steel rebar, however, research on the behavior of concrete confined by both transverse rebar and a steel tube in a circular tube reinforced concrete (CTRC) column is very limited. This research investigates axial response of concrete-filled steel tube or steel jacketed columns considering the confinement effects from rebar and steel tube.

2. Confinement models

Confinement modeling by many researchers such as Ahmad and Shah (1982), Mander *et al.* (1988), and Assa *et al.* (2001) observed that during the axial loading of a reinforced concrete column, as the axial strain increases, the column expands outward while being resisted by the confining hoops or any other reinforcement confining the concrete core. This lateral resistance allows the column to withstand greater volumetric strains and carry larger axial load. The confinement model developed by Mander *et al.* (1988) calculates the lateral confining pressure, f'_l , using Eq. (1) where k_e is the effective confinement coefficient (Eq. (2)) for reinforced concrete.

$$f'_l = \frac{1}{2} k_e \rho_s f_y \quad (1)$$

$$k_e = \frac{\left(1 - \frac{s'}{2d_s}\right)^2}{1 - \rho_{cc}} \quad (2)$$

In Eq. (1), $\rho_s = (4A_{sp}/d_s s)$ where A_{sp} is the cross-sectional area of the transverse rebar hoop or spiral, s is the center-to-center vertical spacing of the rebar, and d_s is the center-to-center distance of the transverse rebar confinement. The parameters s' and ρ_{cc} represent the clear vertical spacing between the lateral steel rebar and the ratio of the area of the longitudinal reinforcement to the area of the concrete core, respectively, and f_y is the yield strength of the rebar. The maximum confined concrete strength, f'_{cc} , is then calculated with Eq. (3) using the lateral confining pressure as well as the unconfined strength, f'_c , obtained from cylinder tests.

$$f'_{cc} = f'_c \left(-1.254 + 2.254 \sqrt{1 + \frac{7.94 f'_l}{f'_c}} - 2 \frac{f'_l}{f'_c} \right) \quad (\text{MPa}) \quad (3)$$

Eq. (4) was also developed by Mander et al. (1988) to calculate the strain at the point of maximum axial load (ε_{cc}) using the confined concrete strength (f'_{cc}), and strain ε_{co} corresponding to the maximum unconfined concrete strength (f'_c).

$$\varepsilon_{cc} = \varepsilon_{co} \left[1 + 5 \left(\frac{f'_{cc}}{f'_c} - 1 \right) \right] \quad (4)$$

O'Shea and Bridge (2000) aimed to modify the Mander *et al.* (1988) model as well as the model developed by Attard and Setunge (1996) to model the load-deformation response of concrete filled tubes (CFTs). The Mander *et al.* (1988) confinement equation with adjusted constants (Eq. (5)) was found to work best for normal strength concrete (50 MPa) while the Attard and Setunge model was found to be a better representative for concrete strengths of 80 MPa and 100 MPa. Eq. (5) uses the empirically derived lateral confining stress formula to calculate p (Eq. (6)) using the unconfined concrete strength f'_c , the yield strength of the steel tube f_y , the thickness of the steel tube t , and the diameter of the steel tube D .

$$f'_{cc} = f'_c \left(-1.228 + 2.172 \sqrt{1 + \frac{7.46 p}{f'_c}} - 2 \frac{p}{f'_c} \right) \quad (\text{MPa}) \quad (5)$$

$$p = p_{yield} \left(0.7 - \sqrt{\frac{f'_c}{f_y}} \right) \left(\frac{10}{3} \right) \quad (\text{MPa}) \quad (6)$$

$$p_{yield} = \frac{2 f_y t}{D} \quad (\text{MPa}) \quad (7)$$

Regardless of the nominal strength of the concrete, a modified Attard and Setunge strain equation (Eq. (8)) is used by O'Shea and Bridge (2000) to determine the strain ε_{cc} at the peak confined concrete strength.

$$\varepsilon_{cc} = \varepsilon_{co} \left(1 + (8 + 0.05 f'_c) \frac{P}{f'_c} \right) \quad (8)$$

The confinement model developed by Mander *et al.* (1988) is useful for predicting the behavior of reinforced concrete columns, but has limited effectiveness when the reinforcement is a steel tube on the outside of the concrete instead of transverse rebar inside the concrete. The confinement model developed by O'Shea and Bridge (2000) is useful when the concrete is confined by a steel tube; however, the range of column diameter to steel tube thickness ratios (D/t) is limited to columns with relatively thinner walls where the D/t ratio is greater than 50. A proposed model will use the mechanics of the Mander *et al.* (1988) model and the modifying approach of O'Shea and Bridge (2000) to predict the load-deformation response of a wider variety of steel tube columns.

3. CFT modelling approach

There are two forms of steel confinement for steel jacketed reinforced concrete columns with the steel tube designated as the primary confinement and the lateral steel rebar designated as the secondary confinement (Fig. 1(b)). It is assumed that the steel jacket acts as the primary form of confinement by confining both cover and core concrete immediately after initial axial loading. As a result of this primary and secondary confinement designation, the steel tube confinement mechanism is evaluated first without the presence of lateral steel. After the existing models are improved for plain concrete filled steel tube columns, the effect of the transverse and longitudinal rebar is evaluated.

Two different types of CFT columns are examined (Fig. 2). The first type (core-series) is a CFT with the axial load applied to the concrete core only. A total of 52 core-series specimens are used in this research. The second type (passive-series) is a CFT loaded similarly to core-series with one

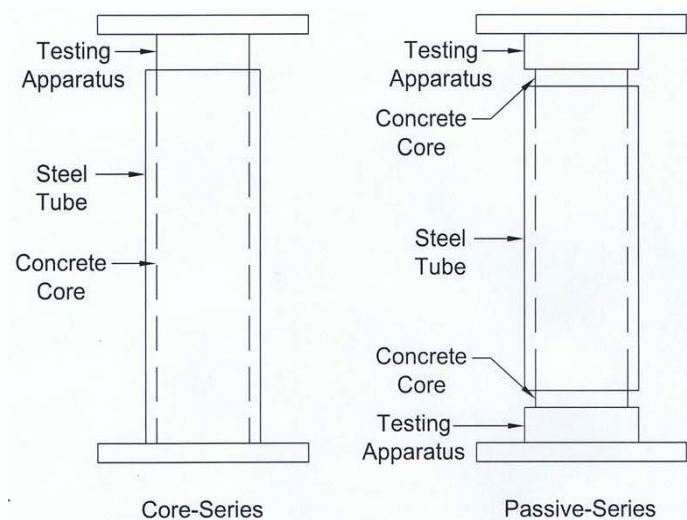


Fig. 2 Core-series and passive-series configuration

important difference. The steel tube of a passive-series column does not fully extend to the bearing ends of the column making the steel tube able to resist only lateral stresses (Fig. 2). The absence of any end-bearing condition for the steel jacket produces a much different behavior under axial loading. Due to the limited availability of experimental data for concentrically loaded circular CTFC columns, the small sample of five passive-series columns is important to the proposed model because the CTFC columns used in this research also have a passive-series configuration. The similar construction of the passive-Series CFT columns and CTFC columns helps in determining the effect of the additional transverse rebar present inside steel tube.

In the nomenclature of the 57 specimens examined, the first letters represent the researchers O'Shea and Bridge (2000), Yu *et al.* (2007), De Oliveira *et al.* (2010), and Liu and Zhou (2010); the first number is the concrete compressive strength; the second number is the steel tube yield strength; the third number is the D/t ratio; the fourth number is the column length-to-column diameter (L/D) ratio and the last part indicated the loading type. Most testing done on CFT columns have focused on modeling short or "stub" columns with a length to diameter ratio of 3. A factor proposed by De Oliveira *et al.* (2010) adjusts the maximum axial load based on a natural logarithmic regression of the length to diameter ratio.

Since a number of the CFT columns in the database considered in this work have an L/D value greater than 3, this factor, $\lambda_{Oliveira}$, in Eq. (9), is applied to all specimens with an L/D ratio larger than 3.

$$\lambda_{Oliveira} = -0.18 \ln\left(\frac{L}{D}\right) + 1.2 \quad (9)$$

The Mander *et al.* (1988) model can be used to allow a continuous steel tube to be modeled as a sequence of closely spaced steel hoops. Two properties used to determine the behavior of the concrete under axial loading is the vertical spacing or spiral pitch of the transverse steel (s) and the clear spacing between the spiral or hoop bars (s'). For CFT specimens used in this research, the steel tube is broken up into 1 mm segments with no clear space between them. This makes the area of the transverse steel equal to the thickness of the tube, t , multiplied by the center-to-center spacing of the 1 mm steel hoops, which is 1 mm. Also, the numerator k_e found using Eq. (2) becomes 1.0.

The effectiveness of existing models was investigated first and then the models and modeling parameters were modified to predict axial behavior of CFT columns. By combining the geometric properties (L , t , and D) and material properties (f'_c and f_y) of the concrete core and steel tube, a non-dimensional property is obtained. This non-dimensional property of the CFT column when plotted against the accuracy of an existing confinement model creates a visible correlation. Fig. 3 shows an increase in the accuracy of the predicted ultimate axial strength as the non-dimensional property increases when using the Mander *et al.* (1988) model. For CFT columns, the model developed by Mander *et al.* (1988) is examined to determine how the model can be improved to better predict the behavior of concrete filled tube columns.

3.1 Development of proposed CFT model strength equations

The first goal in modeling confined concrete is to calculate the confined concrete strength f'_{cc} which is directly related to the confinement effectiveness coefficient, k_e . When the primary confinement mechanism is due to a continuous steel tube, the steel tube behaves differently than lateral steel rebar. All the CFT columns used in this work had their steel tube lateral confining

pressure, $f'_{l,tube}$, adjusted to achieve 100% predicted strength accuracy by multiplying the confinement effectiveness coefficient, k_e , by a modification factor (ϕ_{CFT}), i.e., lateral confinement in Eq. (12) is a modification of Eq. (2). The necessary modification factor for each column was then plotted against the non-dimensional property from Fig. 3 to find a correlation between the non-dimensional property and ϕ_{CFT} are shown in Fig. 4. The equation for the best fit linear line for the 52 core-series specimens is given in Eq. (10). Values for the modified lateral confining pressure of the tube, $f'_{l,tube}$, the modified confined concrete strength, $f'_{cc,CFT}$, the modified predicted ultimate axial load, P_{MAX} , and accuracy of the proposed model for predicting the ultimate axial load, P_{MAX}/P_{Test} , of the core-series columns are all listed in Table 1.

$$\phi_{CFT} = 0.027 \left(\frac{L}{t} \right) \frac{\sqrt{f'_c}}{f_y} + 0.126 \quad (10)$$

For the passive-series CFT columns, the effect of the steel tube acting solely as passive confinement is noticeable when examining the required modifications on the lateral confining pressure. For the five passive-series columns, the adjustment factor, ϕ_{CFT} , is greater than 1.0 based

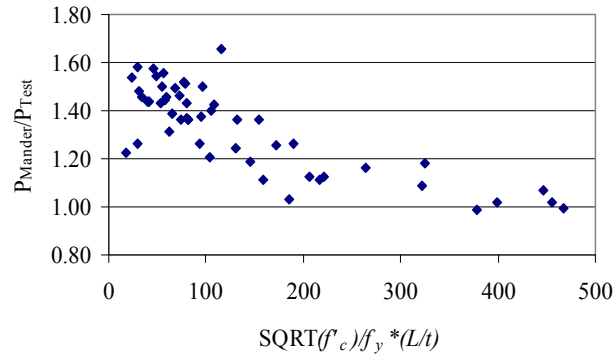


Fig. 3 Effect of combined factors on the accuracy of Mander *et al.* (1988) model

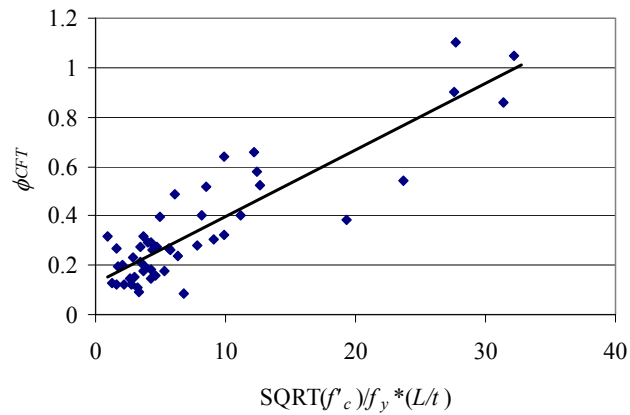


Fig. 4 CFT lateral confining pressure adjustment factor ϕ_{CFT} (Core-Series)

Table 1 Calculated parameters and results from proposed CFT model (Core-Series)

Specimen	$f_{l,tube}^t$ (MPa)	ϕ_{CFT}	$f'_{cc,CFT}$ (MPa)	P_{MAX} (kN)	P_{MAX}/P_{Test}	ϵ_{cc}	ψ_{CFT}	$\epsilon_{cc,CFT}$	$\epsilon_{cc,CFT}/\epsilon_{Test}$
OB-48-363-59-3-C	12.9	0.229	66	1804	1.03	0.0139	8.00	0.0049	–
OB-38-363-59-3-C	12.9	0.219	55	1579	0.96	0.0283	8.00	0.0127	1.06
OB-38-256-98-3-C	5.4	0.348	50	1608	0.97	0.0146	8.00	0.0071	0.90
OB-48-306-125-3-C	5.0	0.392	61	1894	1.03	0.0078	8.00	0.0037	–
OB-38-185-168-3-C	2.2	0.649	47	1404	1.07	0.0093	8.00	0.0044	0.88
OB-38-211-221-3-C	1.9	0.732	47	1388	1.12	0.0104	8.00	0.0044	0.97
OB-56-363-59-3-C	12.9	0.241	75	1973	0.97	0.0127	8.00	0.0049	–
OB-56-256-98-3-C	5.4	0.394	70	2143	0.92	0.0074	8.00	0.0036	–
OB-80-306-125-3-C	5.0	0.469	95	2824	0.98	0.0058	8.00	0.0035	–
OB-56-186-168-3-C	2.2	0.766	68	1943	1.04	0.0045	8.00	0.0032	–
OB-75-211-221-3-C	1.9	0.973	87	2469	1.02	0.0037	8.00	0.0031	–
OB-56-211-221-3-C	1.9	0.870	67	1930	1.00	0.0042	8.00	0.0032	–
OB-77-363-59-3-C	12.9	0.258	98	2419	0.93	0.0147	8.00	0.0076	0.97
OB-77-256-98-3-C	5.4	0.439	92	2740	0.89	0.0057	8.00	0.0042	0.80
OB-77-306-125-3-C	5.0	0.462	92	2734	0.97	0.0063	8.00	0.0045	0.96
OB-77-186-168-3-C	2.2	0.875	90	2548	0.97	0.0039	8.00	0.0032	0.80
OB-108-186-168-3-C	2.2	1.011	123	3441	1.07	0.0034	8.00	0.0029	–
OB-77-211-221-3-C	1.9	0.995	90	2538	0.99	0.0038	8.00	0.0033	0.82
YU-69-350-59-3-C	12.3	0.242	88	2240	1.04	0.0110	8.00	0.0045	–
YU-69-350-60-3-C	12.1	0.244	87	2230	0.99	0.0109	8.00	0.0045	–
ED-33-287-34-3-C	17.9	0.181	51	800	0.98	0.0361	44.62	0.0745	–
ED-59-287-34-3-C	17.9	0.200	80	1067	1.07	0.0263	47.62	0.0390	0.71
ED-89-287-34-3-C	17.9	0.217	113	1365	1.10	0.0206	50.35	0.0180	–
ED-105-287-34-3-C	17.9	0.225	131	1527	0.95	0.0132	51.66	0.0116	0.86
ED-33-343-19-3-C	40.2	0.152	63	1217	0.88	0.0504	39.91	0.1403	–
ED-59-343-19-3-C	40.2	0.161	95	1478	1.04	0.0402	41.32	0.0808	–
ED-89-343-19-3-C	40.2	0.169	129	1759	1.05	0.0328	42.59	0.0395	1.49
ED-105-343-19-3-C	40.2	0.173	147	1910	0.98	0.0213	43.21	0.0271	0.88
ED-33-287-34-5-C	17.9	0.218	54	753	1.00	0.0361	50.51	0.0836	–
ED-59-287-34-5-C	17.9	0.249	85	1009	1.08	0.0263	55.52	0.0446	0.70
ED-89-287-34-5-C	17.9	0.277	119	1292	1.01	0.0206	60.06	0.0206	–
ED-105-287-34-5-C	17.9	0.291	138	1446	0.90	0.0132	62.24	0.0132	0.83
ED-33-343-19-5-C	40.2	0.169	65	1127	0.92	0.0504	42.67	0.1494	–
ED-59-343-19-5-C	40.2	0.184	99	1376	0.99	0.0402	45.01	0.0873	–
ED-89-343-19-5-C	40.2	0.197	134	1643	1.05	0.0328	47.14	0.0430	–

Table 1 Continued

ED-105-343-19-5-C	40.2	0.203	154	1786	0.98	0.0213	48.16	0.0295	1.17
ED-33-287-34-7-C	17.9	0.255	57	724	0.98	0.0361	56.40	0.0927	0.70
ED-59-287-34-7-C	17.9	0.298	89	975	1.05	0.0263	63.41	0.0502	0.78
ED-89-287-34-7-C	17.9	0.338	125	1251	1.04	0.0206	69.77	0.0233	0.81
ED-105-287-34-7-C	17.9	0.357	144	1400	0.93	0.0132	72.83	0.0147	0.91
ED-33-343-19-7-C	40.2	0.186	68	1068	1.07	0.0504	45.43	0.1585	0.81
ED-59-343-19-7-C	40.2	0.207	103	1311	1.05	0.0402	48.71	0.0938	–
ED-89-343-19-7-C	40.2	0.225	140	1571	1.04	0.0328	51.68	0.0465	1.82
ED-105-343-19-7-C	40.2	0.234	160	1710	0.96	0.0213	53.11	0.0320	1.39
ED-33-287-34-10-C	17.9	0.310	61	698	1.24	0.0206	65.24	0.1064	1.04
ED-59-287-34-10-C	17.9	0.372	95	945	1.05	0.0151	75.26	0.0587	1.09
ED-89-287-34-10-C	17.9	0.428	133	1215	1.01	0.0118	84.34	0.0273	1.16
ED-105-287-34-10-C	17.9	0.456	153	1359	0.92	0.0106	88.70	0.0171	1.02
ED-33-343-19-10-C	40.2	0.212	71	1009	1.11	0.0288	49.56	0.1722	1.23
ED-59-343-19-10-C	40.2	0.241	108	1248	1.09	0.0230	54.25	0.1035	–
ED-89-343-19-10-C	40.2	0.268	148	1502	1.08	0.0187	58.49	0.0518	1.37
ED-105-343-19-10-C	40.2	0.280	168	1637	1.02	0.0171	60.54	0.0357	1.21
Average	1.01								
Standard deviation	6.68%								

Table 2 Calculated parameters and results from proposed CFT model (Passive-Series)

Specimen	f'_{Ltube} (MPa)	ϕ_{CFT}	$f'_{cc,CFT}$ (MPa)	P_{MAX} (kN)	P_{MAX}/P_{Test}	ϵ_{cc}	ψ_{CFT}	$\epsilon_{cc,CFT}$	$\epsilon_{cc,CFT}/\epsilon_{Test}$
LZ-59-254-50-3-P	10.2	1.135	1156	1888	0.99	0.0107	0.529	0.0070	0.96
LZ-59-254-70-3-P	7.3	1.232	106	3464	1.02	0.0087	0.567	0.0064	1.10
LZ-59-263-100-3-P	5.3	1.360	99	2971	0.99	0.0071	0.618	0.0061	0.96
LZ-42-254-70-3-P	7.3	1.179	84	2742	1.01	0.0107	0.546	0.0073	1.04
LZ-59-346-70-3-P	9.9	1.142	115	3759	0.99	0.0105	0.531	0.0070	0.96
Average	1.00								
Standard deviation	1.51%								

on Eq. (11) given below where all but two of the core-series specimens have a ϕ_{CFT} less than 1.0. Results similar to the core-series columns' predicted strengths mentioned above are provided for the passive-Series columns in Table 2.

$$\phi_{CFT} = 0.0053 \left(\frac{L}{t} \right) \sqrt{\frac{f'_c}{f_y}} + 0.894 \quad (11)$$

The lateral confining pressure of the steel jacket was calculated using Eqs. (12) and (13).

$$f'_{l,tube} = \frac{1}{2} k_e \alpha f_y \phi_{CFT} \quad (12)$$

$$\alpha = \frac{4t}{D_c} \quad (13)$$

where D_c is the diameter of the plain concrete core. The confined concrete strength of the CFT column, $f'_{cc,CFT}$, is obtained by modifying the Mander *et al.* (1988) constants from Eq. (3) with the new lateral confining pressure value, $f'_{l,tube}$, as given below.

$$f'_{cc,CFT} = f'_c \left(-1.254 + 2.254 \sqrt{1 + \frac{7.94 f'_{l,tube}}{f'_c}} - 2 \frac{f'_{l,tube}}{f'_c} \right) \quad (14)$$

Through the use of the modification factor, ϕ_{CFT} , the lateral confining pressure of the steel tube is adjusted to account for the local buckling behavior of the steel for the core-series. Without this modification factor, the steel tube is assumed to be uniformly loaded in the transverse direction only. Therefore, by using ϕ_{CFT} , more accurate predictions are obtained while maintaining similar mechanics of concrete column behavior. The adjusted lateral confining pressure is then used to calculate a more accurate confined concrete strength.

3.2 Development of Proposed CFT Model Strain Equations

In the Mander *et al.* (1988) model, it is necessary to determine the strain ($\epsilon_{cc,CFT}$) at the point of maximum confined concrete strength ($f'_{cc,CFT}$). The value of $\epsilon_{cc,CFT}$ is calculated in this work by replacing the constant “8.0” in Eq. (8) with the factor (ψ_{CFT}) using the same non-dimensional property in Fig. 4 for the 32 core-series columns with a D/t value less than 50. Fig. 5 shows the correlation between the modification factor and the non-dimensional property for the plain concrete-filled thick-steel-walled columns used in this research.

The best fit line for the data in Fig. 5 from the 22 thick walled CFT core-series columns examined is given below (Eq. (15)). The coefficient ψ_{CFT} is used in Eq. (16) to calculate the strain corresponding to the peak strength. Of the 10 columns not included in the derivation of Eq. (15), six columns did not have complete data sets showing the strain at the point of maximum load, and four columns were clear outliers due to extreme displacements. Details of derivation of Eqs. (15) and (16) and discussion of test data are provided in Rupp (2012).

$$\psi_{CFT} = 4.34 \left(\frac{L}{t} \right) \frac{\sqrt{f'_c}}{f_y} + 35.78 \quad (15)$$

$$\epsilon_{cc,CFT} = \epsilon_{co} \left[1 + (\psi_{CFT} + 0.05 f'_{co}) \left(\frac{p}{f'_c} \right) \right] \quad (16)$$

The remaining 20 core-series thin-walled specimens do not follow the same correlation as the 32 core-series thick-walled specimens. These thin-walled specimens have a D/t greater than or equal to 50 and they do not behave in a similar manner as the thicker tube CFT columns. Therefore, Eq. (8) developed by O'Shea and Bridge (2000) can be used to predict the strain at peak

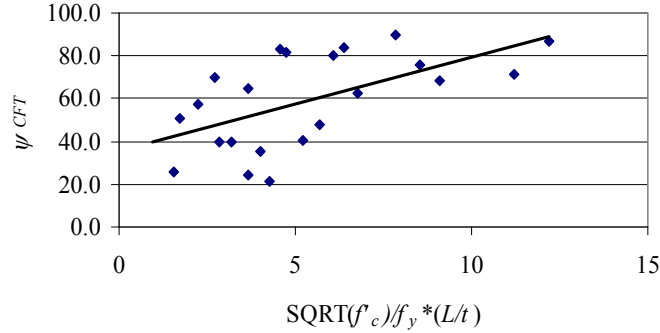


Fig. 5 Variation of peak strain factor, ψ_{CFT} , for CFT Specimens with $D/t < 50$

strength ($\varepsilon_{cc,CFT}$) for the thin-walled CFT core-series columns (ψ_{CFT} in Eq. (16) is equal to 8.0 in Eq. (8)). The values of the modified predicted corresponding strain at the point of ultimate axial strength and the accuracy of the proposed model for predicting the corresponding strain, $\varepsilon_{cc,CFT}/\varepsilon_{Test}$, of the core-series columns are listed in Table 1.

For the passive-series columns, the strain prediction at peak load, $\varepsilon_{cc,CFT}$, is calculated by modifying the Mander *et al.* (1988) strain equation (Eq. (4)). The passive-series peak strain modification factor, ψ_{CFT} , can be calculated using Eq. (17). Eq. (18) is used to calculate the strain at peak strength for passive-series columns. The strain predictions are provided for the passive-series columns in Table 2.

$$\psi_{CFT} = 0.021 \left(\frac{L}{t} \right) \frac{\sqrt{f'_c}}{f_y} + 0.434 \quad (17)$$

$$\varepsilon_{cc,CFT} = \varepsilon_{co} \left[1 + (5.0\psi_{CFT}) \left(\frac{f'_{cc,CFT}}{f'_c} - 1 \right) \right] \quad (18)$$

By using the strain modification factor, ψ_{CFT} , the axial deformation capacity at the point of maximum axial loading is more accurately predicted for concrete-filled tube columns with diameter-to-thickness ratios less than 50. The formula by O'Shea and Bridge (2000) is still used for thinner walled CFT columns with diameter-to-thickness ratios greater than or equal to 50 (Eq. (8)). The modification factor shows the increased deformation capacity of CFT columns while not affecting the mechanics of the original model equations.

The secant modulus for the confined concrete, E_{sec} , is the parameter used to define the slope of the ascending branch of the confinement stress-strain diagram. It's value can be determined by dividing the peak confined concrete strength, f'_{cc} , by the strain value corresponding to the maximum strength, ε_{cc} . ($E_{sec} = f'_{cc}/\varepsilon_{cc}$). When calculating the ultimate axial strength of CFT columns, the unadjusted confined concrete strength and peak strain values, ignoring the effects of ϕ_{CFT} and ψ_{CFT} , are used to calculate the secant modulus for core-series CFTs using Eqs. (3) and (8). For passive-series CFTs, the adjusted confined concrete strength and peak strain values are obtained from Eqs. (14) and (18). Fig. 6 shows the flow chart for the proposed procedure of modeling the axial capacity (P_{MAX}) of a concrete filled tube column as a function of uniform axial strain (ε_c or ε_s) or axial displacement ($\Delta = \varepsilon \cdot L$).

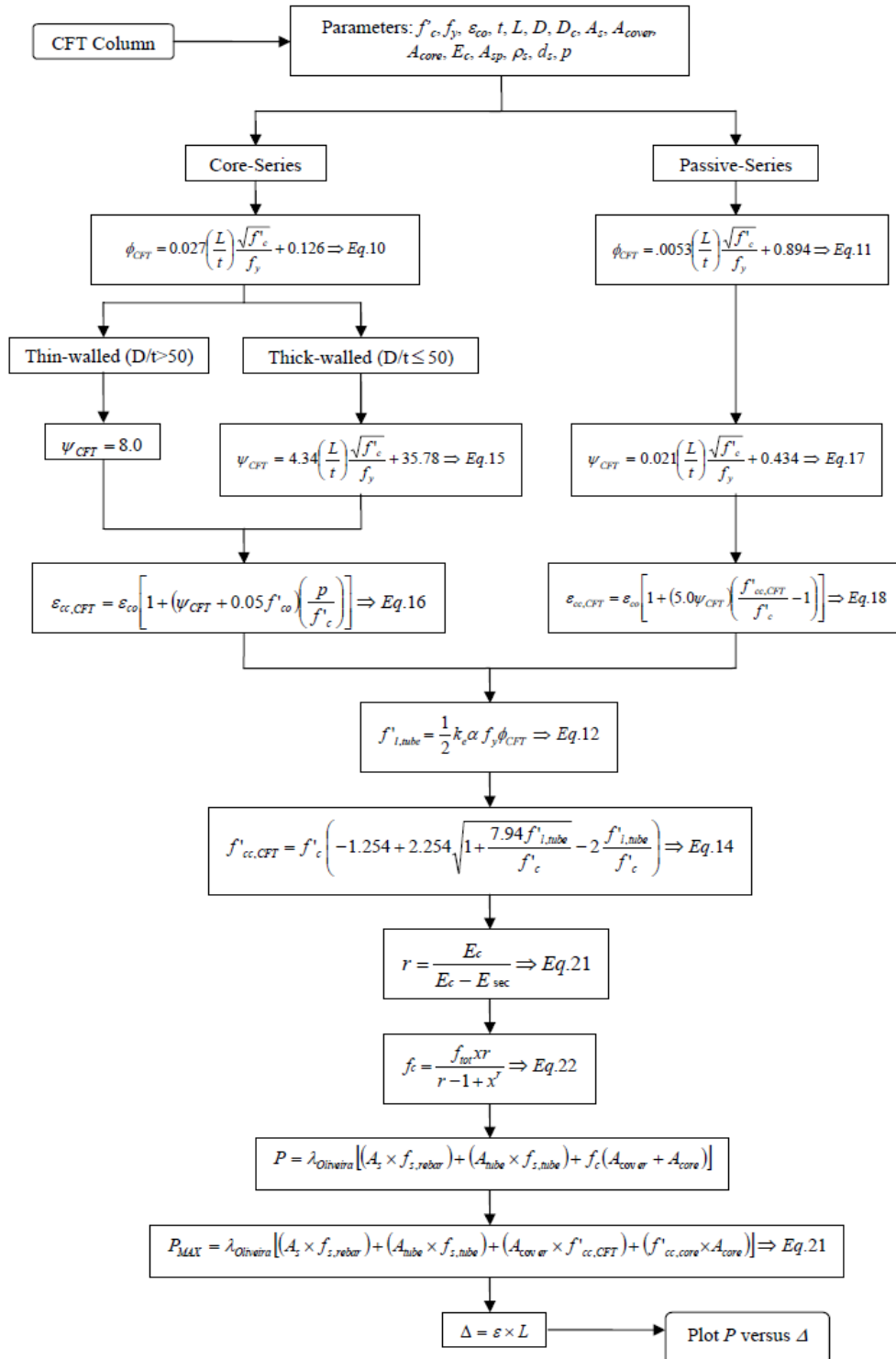


Fig. 6 Flow diagram for the proposed model to calculate the axial capacity of concrete-filled steel tube columns

4. Steel tube jacketed reinforced concrete behavior

The proposed CFT model with modification factors ϕ_{CFT} and ψ_{CFT} provides a more accurate base model for Circular Tube confined Reinforced Concrete (CTRC) columns. Five CTRC columns with available research data tested by Liu and Zhou (2010) are used to understand the change in behavior of a CFT column when transverse rebar reinforcement is present (Table 3). Five other columns, the passive-series, used in this research were also tested by Liu and Zhou (Table 2). Both CTRC columns and passive-series columns had similar test setup.

To calculate the inner core confined concrete strength (Eq. (19)) for CTRC columns, the CFT confined concrete strength $f'_{cc,CFT}$ from Eq. (14) is substituted for the unconfined concrete strength f'_c in Eq. (3). This is because the proposed model assumes that the core concrete is confined by the steel jacket before the transverse rebar effectively confines the inner concrete core. The confined concrete strength of the inner core $f'_{cc,core}$ confined by the lateral rebar is calculated by determining the effect that the lateral confining pressure from the rebar f'_l (Eq. (1)) has on the already confined inner concrete core.

$$f'_{cc,core} = f'_{cc,CFT} \left(-1.254 + 2.254 \sqrt{1 + \frac{7.94 f'_l}{f'_{cc,CFT}}} - 2 \frac{f'_l}{f'_{cc,CFT}} \right) \quad (19)$$

The confined concrete strength of the inner core is multiplied by the area of the inner concrete core and added to the product of the CFT confined concrete strength and cover concrete area, the product of the steel tube area and steel tube yield strength, and the longitudinal rebar area and rebar yield strength (Eq. (21)). This axial load capacity is multiplied by $\lambda_{Oliveira}$ (Eq. (9)) to account for the slenderness of the column if L/D is greater than 3.

$$P = \lambda_{Oliveira} \left[(A_s \times f_{s,rebar}) + (A_{tube} \times f_{s,tube}) + f_c (A_{cover} + A_{core}) \right] \quad (20)$$

$$P_{MAX} = \lambda_{Oliveira} \left[(A_s \times f_{s,rebar}) + (A_{tube} \times f_{s,tube}) + (A_{cover} \times f'_{cc,CFT}) + (f'_{cc,core} \times A_{core}) \right] \quad (21)$$

Liu and Zhou (2010) concluded from the tests of five passive-series CFT columns (Table 2) and five similar CTRC columns (Table 3) that the presence of the rebar inside the concrete core has very little effect on the peak longitudinal strain of the column as well as on the overall column stiffness. Based on this conclusion, no additional modifications are required to calculate the strain at maximum load or the secant modulus for CTRC columns. In conclusion, the lateral steel rebar added to the CFT columns increases the maximum axial strength and has minimal effect on the peak strain and stiffness. Peak strength, strain, and associated parameters are listed in Table 3 for the five CTRC columns tested by Liu and Zhou (2010).

To calculate the load versus displacement curves in Fig. 7, Eqs. (22) and (23) proposed by Mander *et al.* (1988) are used where $x = \epsilon_c / \epsilon_{cc,CFT}$ and E_c equals the modulus of elasticity for the concrete core. For core-series columns, the unmodified confined concrete strength and peak strain values are used to calculate the secant modulus ($E_{sec} = f'_{cc} / \epsilon_{cc}$) while the modified strength and strain values are used for passive-series columns, ($E_{sec} = f'_{cc,CFT} / \epsilon_{cc,CFT}$).

$$r = \frac{E_c}{E_c - E_{sec}} \quad (22)$$

$$f_c = \frac{f_{tot} x^r}{r - 1 + x^r} \tag{23}$$

In Eq. (23), f_{tot} is the equivalent uniform stress over the entire cross-sectional area of the concrete, A_c , area of the steel tube, A_{tube} , and area of the longitudinal steel rebar, A_s . For passive-series columns, A_{tube} is equal to zero due to the steel tube’s capacity to resist transverse load and not axial load.

In Figs. 7 through 9, the axial column displacements Δ (or the x -axis values) are calculated by multiplying the height of column specimens with the axial strain, ϵ values. This is shown as $\Delta = \epsilon \times L$ in Fig. 6. Axial strain ϵ is varied from zero to maximum strain where the confined concrete crushes at a strain value of ϵ_{cc} ($\epsilon_{cc,CFT}$ in Eq. (16) or (18)).

The vertical axis in Figs. 7 through 9 indicates the axial load P . Total axial load resisted by each column is calculated from Eq. (20) or (21) as illustrated in Fig. 6. Essentially the total axial load is the sum of axial resistances by the steel rebar (rebar stress times rebar cross sectional area

Table 3 Stresses, axial loads and strains calculated from the proposed CTRC model

Specimen	$f'_{l,tube}$ (MPa)	ϵ_{CFT}	$f'_{cc,CFT}$ (MPa)	$f'_{cc,core}$ (MPa)	P_{MAX} (kN)	P_{MAX}/P_{Test}	ϵ_{cc}	ψ_{CFT}	$\epsilon_{cc,CFT}$	$\epsilon_{cc,CFT}/\epsilon_{Test}$
LZ-59-254-50-3-RC	10.2	1.135	116	116	1973	0.96	0.0107	0.529	0.0070	0.85
LZ-59-254-70-3-RC	7.3	1.232	106	107	3651	0.98	0.0087	0.567	0.0064	1.01
LZ-59-263-100-3-RC	5.3	1.360	99	100	3145	0.93	0.0071	0.618	0.0061	1.08
LZ-42-254-70-3-RC	7.3	1.179	84	85	2929	1.05	0.0107	0.546	0.0073	1.28
LZ-59-346-70-3-RC	9.9	1.142	115	116	4003	0.98	0.0105	0.531	0.0070	1.05
Average						0.98				
Standard deviation						4.69%				

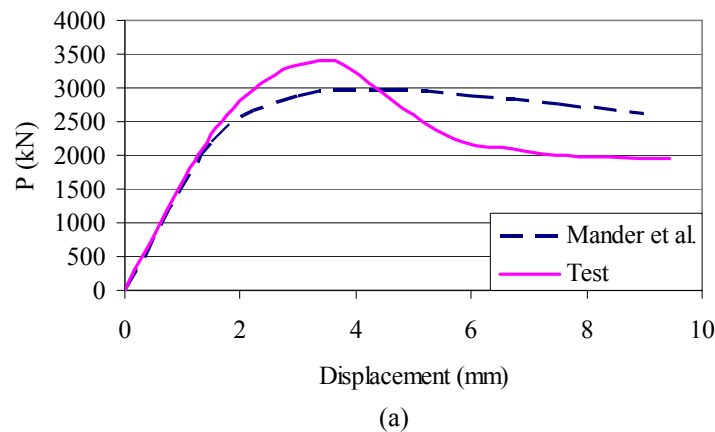
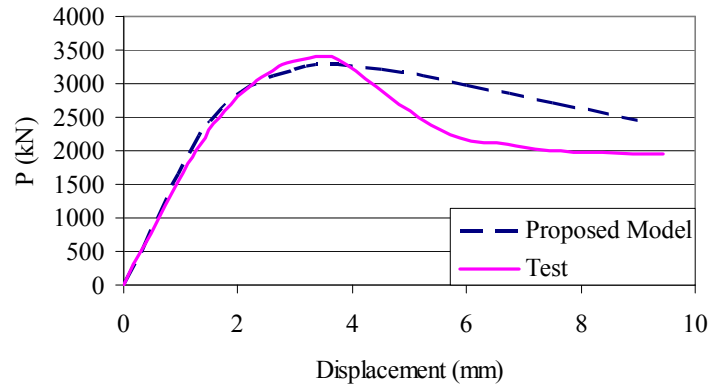


Fig. 7 Calculated and experimental load versus displacement relation for LZ-59-263-100-3-RC with Mander *et al.* (1988) model and proposed CTRC model



(b)

Fig. 7 Continued

$A_s \times f_{s,bar}$), steel tube ($A_{tube} \times f_{s,tube}$), and cover and core concrete ($[f_c(A_{cover} \times A_{core})]$), where concrete strength f_c is calculated from Eq. (23)).

5. Model evaluation and comparison of results

The use of the modification factors increases the accuracy of the predicted ultimate axial capacity of the column, the displacement at maximum axial load, and the rate at which the column is vertically displaced. Experimental data from 52 CFT and 5 CTRC specimens were used to develop the proposed axial response model. Figs. 8 and 9 compare the experimental behavior of a core-series and passive-series CFT column with the response predicted by the proposed CFT

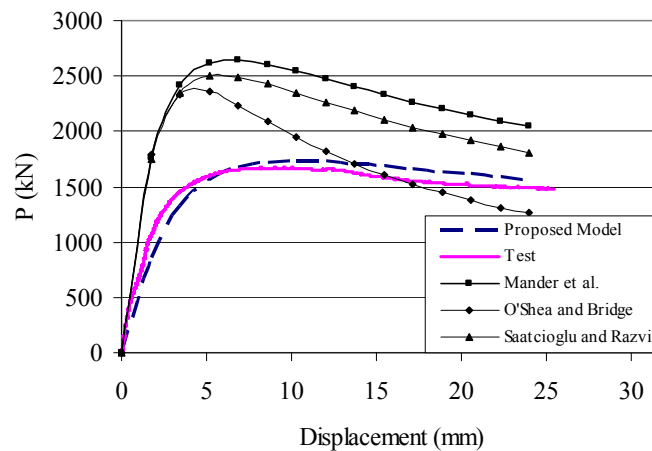


Fig. 8 Experimental and predicted response of ED-89-343-19-3-C

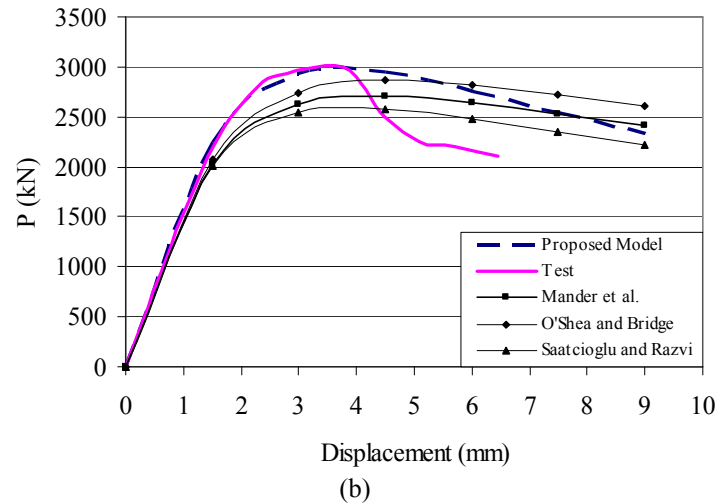


Fig. 9 Experimental and predicted response of LZ-59-263-100-3-P

model, and Mander *et al.* (1988), O'Shea and Bridge (2000), and Saatcioglu and Razvi (1992) models. Eq. (23) developed by Mander *et al.* is used for all the models to plot the load versus displacement behavior. Calculated load-displacement responses of all columns can be found in Rupp (2012).

For core-series specimens, Fig. 8 shows how existing confinement models consistently overestimate the initial stiffness and ultimate axial capacity of the column while underestimate the strain at the point of ultimate axial load. The proposed model is much more accurate with all three aspects of the load versus displacement behavioral curve by taking into consideration the behavior of the continuous steel jacket under biaxial stresses.

Fig. 9 shows that passive-series specimens behave similar to reinforced concrete columns and, as a result, the existing confinement models predict a relatively accurate load-displacement response. The difference in behavior of core-series and passive-series columns under concentric axial loads is most apparent when Figs. 8 and 9 are compared. The modifications in the proposed model are not as significant for passive-series columns as they are for core-series columns because the existing confinement models predict the response relatively accurately.

6. Conclusions

A new model is proposed to calculate axial load-displacement behavior for concrete-filled steel tubes and steel tube jacketed reinforced concrete columns. Evaluation of experimental data from a large number of column specimens showed that the lateral steel rebar added to the CFT columns increases the maximum axial strength however has minimal effect on the peak strain and stiffness.

Using the Mander *et al.* (1988) model as a basis the lateral confining pressure (f'_l) was modified using a new factor ϕ_{CFT} , and the peak strain at the point of maximum load (ϵ_{cc}) was modified using another new factor ϕ_{CFT} . For core-series columns, the modified O'Shea and Bridge (2000) strain equation is used while the Mander *et al.* (1988) strain equation is used for passive-series columns.

The results of the proposed CFT model show an improved accuracy in predicted strength within 1.0% with a standard deviation of 6.4%. The predicted peak strain values are not as accurate, overestimated by less than 1.0% with a higher standard deviation of 24.2% with four test specimen outliers. These inaccuracies can be attributed to the unknown unconfined concrete peak strain values, ϵ_{co} , as well as the manner in which the experimental strains were measured and gathered.

Based on the proposed CTRC model, the predicted strength for the five CTRC columns is only 1.8% underestimated with a standard deviation of less than 5.0% while the strain values predicted within 6.0% with a standard deviation of approximately 15.1%. The number of available test data for CTRC columns is very limited and further research needs to be performed to help determine the effectiveness of a steel jacket on transverse rebar inside the column. In addition to more testing on CTRC columns, testing should be performed on axially pre-loaded concrete columns with new confinement jackets. The proposed model in this paper is better suited for brand new concrete columns wrapped in steel jackets or concrete-filled steel tubes. Similar to other confinement models, it is assumed that the transverse rebar is not yet under any form of lateral stress at the point of initial loading. However, for many retrofitted columns, the lateral reinforcement is under significant stress and will continue to be laterally stressed during the retrofitting process or in new concrete filled steel tubes.

References

- Ahmad, S.H. and Shah, S.P. (1982), "Stress-strain curves of concrete confined by spiral reinforcement", *ACI J.*, **79**(6), 484-490.
- Assa, B., Nishiyama, M. and Watanabe, F. (2001), "New approach for modeling confined concrete. I: Circular columns", *ACI Struct. J.*, **127**(7), 743-750.
- Attard, M.M. and Setunge S. (1996), "Stress-strain relationship of unconfined and confined concrete", *ACI Mater. J.*, **93**(5), 432-441.
- De Oliveira, W.L.A., De Nardin, S., El Debs, A.L.H. and El Debs, M.K. (2010), "Evaluation of passive confinement in CFT columns", *J. Construct. Steel Res.*, **66**(4), 487-495.
- Giakoumelis, G. and Lam, D. (2004), "Axial capacity of circular concrete-filled tube columns", *J. Construct. Steel Res.*, **60**(7), 1049-1068.
- Gupta, P.K., Sarda, S.M. and Kumar, M.S. (2007), "Experimental and computational study of concrete filled steel tubular columns under axial loads", *J. Construct. Steel Res.*, **63**(2), 182-193.
- Hatzigeorgiou, G.D. (2008), "Numerical model for the behavior and capacity of circular CFT columns, part I: theory", *Eng. Struct.*, **30**(6), 1573-1578.
- Knowles, R.B. and Park, R. (1969), "Strength of concrete-filled steel tubular columns", *J. Struct. Div.*, **95**(12), 2565-2587.
- Liu, J. and Zhou, X. (2010), "Behavior and strength of tubed RC stub columns under axial compression", *J. Construct. Steel Res.*, **66**(1), 28-36.
- Mander, J.B., Priestley, M.J.N. and Park, R. (1988), "Theoretical stress-strain model for confined concrete", *ASCE J. Struct. Eng.*, **114**(8), 1804-1826.
- O'Shea, M.D. and Bridge, R.Q. (2000), "Design of circular thin-walled concrete filled steel tubes", *ASCE J. Struct. Eng.*, **126**(11), 1295-1303.
- Rupp, J. (2012), "Modeling of steel-jacketed reinforced concrete under axial compressive loads", *Master's Thesis*, The Ohio State University, Columbus, OH, p. 211.
- Saatcioglu, M. and Razvi, S.R. (1992), "Strength and ductility of confined concrete", *ASCE J. Struct. Eng.*, **118**(6), 1590-1607.
- Sakino, K., Nakahara, H., Morino, S. and Nishiyama, I. (2004), "Behavior of centrally loaded concrete-filled

- steel-tube short columns”, *ASCE J. Struct. Eng.*, **130**(2), 180-188.
- Sezen, H. and Miller, E.A. (2011), “Experimental evaluation of axial behavior of strengthened circular reinforced-concrete columns”, *ASCE J. Bridge Eng.*, **16**(2), 238-247.
- Sezen, H. and Shamsai, M. (2008), “High-strength concrete columns reinforced with prefabricated cage system”, *ASCE J. Struct. Eng.*, **134**(5), 750-757.
- Yu, Z., Ding, F. and Cai, C.S. (2007), “Experimental behavior of circular concrete-filled steel tube stub columns”, *J. Construct. Steel Res.*, **63**(2), 165-174.
- Zhong, S.T. and Miao, R.Y. (1987), “Stress-strain relationship and strength of concrete filled tubes”, *Composite construction in Steel and Concrete, Proceedings of Engineering Foundation Conference*, pp. 773-785.

CC